Proceedings of the 37th Annual Conference of the IEEE Industrial Electronics Society (IECON 2011), Melbourne, Australia, November 7-10, 2011.

# A Hybrid Bearing Concept for High-Speed Applications Employing Aerodynamic Gas-Bearings and a Self-Sensing Active Magnetic Damper

A. Looser
J. W. Kolar

# A Hybrid Bearing Concept for High-Speed Applications Employing Aerodynamic Gas-Bearings and a Self-Sensing Active Magnetic Damper

A. Looser and J.W. Kolar
Power Electronic Systems Laboratory
ETH Zurich
CH-8092 Zurich, Switzerland
looser@lem.ee.ethz.ch

***Abstract*—Successful application of ultra high-speed electrical drive systems in industrial products is currently limited by lacking high-speed bearing technologies permitting high reliability and long lifetime. Promising bearing technologies for high rotational speeds are contact-less bearing concepts such as active magnetic bearings or gas bearings. While magnetic bearings usually are major electromechanical systems with substantial complexity, gas bearings allow compact realizations with high load capacity and stiffness; however poor dynamic stability has been limiting their use at high rotational speeds. For a new hybrid bearing concept employing an aerodynamic gas bearing for load support, a small-sized self-sensing active magnetic damper is proposed allowing to effectively counteract the self-excited whirl instability of the gas bearing and therewith enabling high speed operation with a minimum of additional complexity and costs.**

## I. Introduction

The use of todays ultra high-speed electrical drive systems in industrial applications has been limited mainly by the absence of reliable bearings for rotor support. Precision ball bearings designed for dental drills with a maximum rotational speed of $400\ \mathrm{krpm}$ showed a total lifetime of around 200 to 300 hours in cyclic tests where the speed was varied between $200\ \mathrm{krpm}$ and $500\ \mathrm{krpm}$. However, for potential industrial high-speed applications such as turbo-compressors used in heat pumps, fuel cells or cryogenics a lifetime of several years at speeds beyond $500\ \mathrm{krpm}$ would be required. Promising candidates for high-speed bearings with longer lifetimes are contact-less concepts such as the active magnetic bearing or the gas bearing, where the rotor is carried by the fluid film generated between the bearing bush and the journal. For aerodynamic bearings the fluid film is generated by the journal rotation itself, therewith eliminating the need of an external pressurized air supply and allowing for a very compact design. Usually, gas bearings can be designed much smaller than magnetic bearings for the same load capacity and stiffness, for which reason more compact drive systems can be realized. Another advantage is the reduced system complexity due to the absence of position sensors, power amplifiers and control as used in classical magnetic bearing designs.

One of the major challenges with high speed gas bearings however is the self-excited whirl instability which limits the maximum operating speed. The phenomenon of whirl instability has been known from the beginning of fluid film lubrication and has been thoroughly studied e.g. in [1]. The main causes for the instability are a destabilizing azimuthal force component vertical to the journal displacement, instead of a purely radial force into the bearing center, combined with relatively low damping from the fluid film itself. Increasing the rotor weight additionally worsens stability. Although the amount of damping within the fluid film itself theoretically could be increased even for very high speed operation e.g. when scaling the bearing geometry and allowing for a smaller bearing clearance, this method is hardly practicable because of the requirement for very high precision fabrication which finally would limit an industrial implementation.

Bearing types with improved stability are the pivoted-pad or tilting-pad bearing [2]. Also herringbone grooved bearings, which have the advantage of a much simpler fixed geometry, have shown good stability [3]. Both bearing types reduce the destabilizing force and therefore allow for higher speeds before becoming unstable. Also foil bearings show improved stability mainly due to introduced damping within the foil layers. With foil bearings, speeds up to $700\ \mathrm{krpm}$ have been reported, however driven by a relatively light air turbine [4]. Rotational speeds as high as $1.2\ \mathrm{Mrpm}$ have been achieved using a flexible o-ring supported bearing bush with an oil damper [5]. However with the elastic support, also the overall stiffness of the bearing-damper assembly is reduced significantly. In [6] an active magnetic bearing is employed in order to control the oil whirl and oil whip instability of a journal bearing and therewith increase the range of operation.

It can be summarized that generally there have been two strategies to improve the bearings stability. Improvements have been achieved either by a reduction of the destabilizing azimuthal force component usually accomplished by a special bearing geometry, or by the introduction of additional damping from outside the fluid film or a combination of both.

For many applications the bearings are supposed to support a rotor of an electrical machine capable of providing the required shaft power for the application. The rotor of such a system will probably be heavier than the air-turbines used

978-1-61284-972-0/11/$26.00 ©2011 IEEE

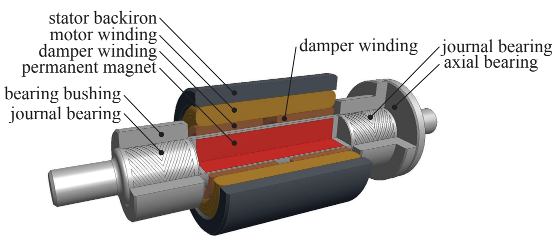


Fig. 1. CAD Drawing of the high-speed drive system with permanent magnet rotor, gas bearings and windings for the motor and dampers

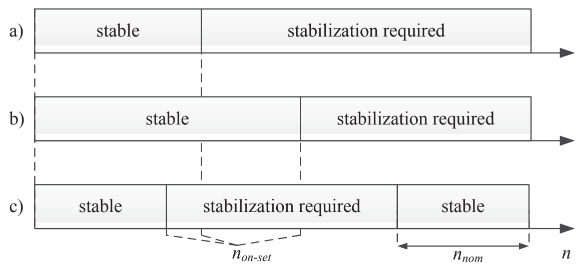


Fig. 2. Stable regions and required stabilization by means of external damping for a) conventional HGJB with constant groove angle, b) HGJB with curved grooves optimized for maximum uninterrupted stability region, c) HGJB with curved grooves optimized for maximum stability in nominal speed region

for high-speed bearing tests in some of the above mentioned approaches and therefore a bearing with even better stability will be required.

In this work, a small-sized self-sensing electromagnetic damper acting directly on the rotor is proposed which enables stable operation at high speed without compromising the gas bearing load capacity or stiffness. First, the drive system including motor, gas bearing and magnetic damper is described in section II. The rotor position self-sensing method employing a high frequency sinusoidal signal injection approach is described in section III. Finally, in section IV experimental results for the radial rotor position sensing are presented.

## II. System Description

The electrical motor is a slot-less type permanent magnet synchronous machine constructed similar to the machine in [7], which has been well-proven for high rotational speeds. An overview on the planned system is given in Fig. 1. The rotor consist of a diametrically magnetized permanent magnet encased in a retaining sleeve to protect the brittle permanent magnet from breaking due to the high centrifugal forces at high speeds. For both the motor winding and the damper winding, slot-less type air-gap windings with litz wire are used in order to minimize the eddy current losses caused by the permanent magnet field at high frequencies. For the same reason, the stator back iron consists of amorphous iron.

A spiral-grooved axial gas bearing is used for axial rotor support while herringbone-grooved journal bearings (HGJB) provide the radial support. For axial bearings, instable behavior is much less a concern than for the journal bearings. Therefor no magnetic dampers are required for axial stabilization. State-of-the-art HGJBs using a simple groove geometry with constant groove angle become unstable for speeds beyond the so-called self-excited instability on-set speed ($n_{on\text{-}set}$) and the required amount of damping for stabilization would then increase with speed. Calculations have shown that when using curved grooves, i.e. non constant groove angles, the stability of the bearing can be improved and less external damping will be required at high speed. Moreover by optimizing the groove geometry the dynamic response of the bearing can be shaped such that stable operation is obtained again beyond the first instability on-set speed. For such a bearing instability might occur already at lower speeds without external damping, however for the stable region at high speed no external damping will be required. Fig. 2 qualitatively illustrates the bearing stability behavior and damping strategies for the optimized bearings with improved stability region and the split stability region in comparison to the conventional bearing with constant groove angle. For applications such as turbo-compressors, which are mainly operated in a relatively narrow range around nominal speed $n_{nom}$, the bearing could be designed to have a stable region at nominal speed and therefore no external damping would be required during normal operation. Only for passing through the unstable region during start-up and run-down external damping will be required for a short time, which allows for a very small magnetic damper design without affecting the overall efficiency at nominal speed.

Generally both a homopolar and a heteropolar damper topology would be suited for vibration control of a shaft rotating at high speeds. The concepts homopolar and heteropolar describe magnetic bearing configurations, where the term heteropolar refers to a configuration where the rotor is exposed to a magnetic field with alternating polarity as it rotates and the term heteropolar denotes a configuration with unchanging polarity [8]. For a heteropolar realization of the magnetic damper, an additional air-gap winding with the same diametrically magnetized permanent magnet on the rotor as is already needed for drive torque generation is used, similar to the magnetic bearing described in [9]. The force generation principle with such an air-gap winging is visualized in Fig. 3. The inner winding is used to produce a fundamental current distribution with a pole pair number of two, hence with the magnetic field of diametrically magnetized permanent magnet, Lorentz forces act on the winding, respectively a resultant reaction force is obtained on the rotor. The outer winding with only one pole pair produces a force couple, therefore a torque results on the rotor. For such a heteropolar realization using the same permanent magnet for both force and torque generation, the gas bearings are located outside the motors active region as depicted in Fig. 1.

As an option, arranging the damper at the same place as the gas bearings increases the distance of the dampers to the rotor center of gravity and therewith brings the advantage of an improved effectiveness in damping in the case of a conical mode whirl, however both the sensitivity for position

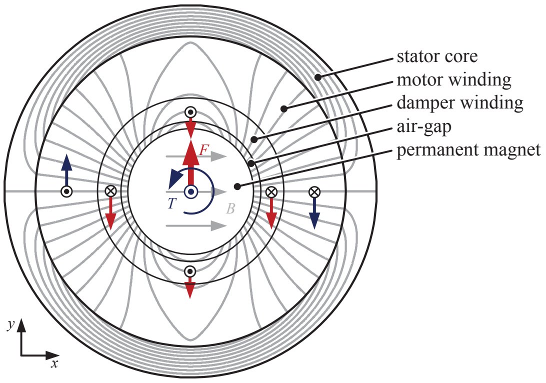


Fig. 3. Force and torque generation principle for the motor and the damper winding.

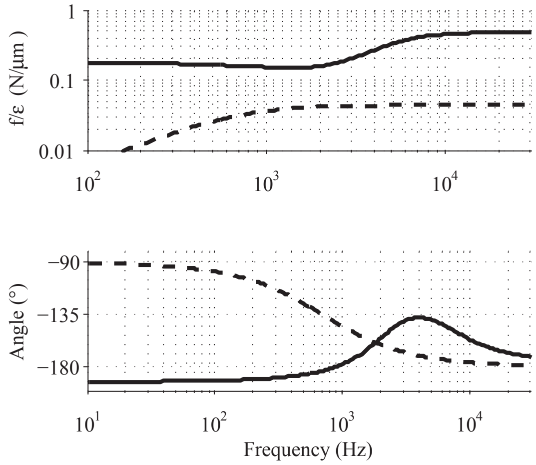


Fig. 4. Bode diagram of the dynamic stiffness ($f/\varepsilon$) and its phase angle for the gas bearing (solid line) and the damping force provided by the magnetic damper (dashed line), which is needed to stabilize the rotor in the unstable region around 300 krpm.

sensing and the amount of producible force is decreased because of the increased magnetic air-gap introduced with the necessary bearing bushing between the rotor and the windings. Naturally to avoid excessive losses due to eddy currents and not to impede position self-sensing, the material of the bearing bushing would need to be non-conductive, such as e.g. glass ceramics.

For a homopolar realization additional permanent magnets are needed to generate a uniform radial field in the damper winding, achieved with e.g. axially magnetized permanent magnets. Therefor, with the different magnetization direction of the permanent magnets required for the dampers and the motor, the dampers cannot be integrated into the active region of the motor. Arranging the dampers at the locations of the gas bearings and placing additional permanent magnets into the bearing journal is advisable in spite of the above mentioned decrease in sensitivity and producible force, because additional rotor length and weight can be avoided and because of the improved damper effectiveness in a conical mode whirl. However, because of the better integration of damper and motor only the heteropolar concept is considered further.

The damper forces in the two radial directions $x$ and $y$ can be described as

$$f_x = K_I \cdot i_d \tag{1}$$

$$f_y = K_I \cdot i_q, \tag{2}$$

where $K_I$ is the force-current constant of the damper and $i_d$ and $i_q$ are the transformed currents in the rotating coordinate system of the rotor. The rotating $dq$ coordinate system is defined by the rotor angle $\theta_r$, which is given by the direction of the permanent magnet flux (Fig. 5). Based on the radial velocity in the according directions

$$v_x = \frac{\mathrm{d}}{\mathrm{d}t}\varepsilon_x \tag{3}$$

$$v_y = \frac{\mathrm{d}}{\mathrm{d}t}\varepsilon_y, \tag{4}$$

expressed in terms of the journal displacements $\varepsilon_x$ and $\varepsilon_y$, the damping control reference currents are given by

$$i_d^* = -\frac{d}{K_I} \cdot v_x \tag{5}$$

$$i_q^* = -\frac{d}{K_I} \cdot v_y, \tag{6}$$

where $d$ is the damping constant. For vibrations with high frequencies the above time derivative would yield very high damper currents. Therefore, a first order low pass filter is applied, limiting damping at approximately 1 kHz. For a bearing with curved grooves, optimized with a split stability region (Fig. 2c) supporting a rotor with a total mass of 12 g at a maximum speed of 500 krpm without external damping, the resulting damping forces required to stabilize the rotor in the unstable region around 300 krpm is plotted in the Bode diagram in Fig. 4. For comparison, the dynamic stiffness of the gas bearing with a diameter of 6 mm, a length of 8 mm and a clearance of 15 $\mu$m is also shown. The dynamic stiffness of the gas bearing has been calculated using a finite difference method to solve the partial differential equation for the average pressure which is based on the narrow groove theory originally proposed in [10]. Compared to the force provided by the gas-bearing, the required damping force is relatively small. Also note, that the rotor displacements $\varepsilon$ are not necessarily the same at the place of the bearing or of the damper, hence in the case of a conical whirl mode the absolute forces provided by the damper are even smaller due to the shorter distance to the rotor center. As a result of the only small required forces, the magnetic dampers can be designed significantly smaller compared to a drive system with magnetic bearings providing the full rotor support.

## III. Position Sensing - High Frequency Signal Injection

In order to produce damping forces in response to radial rotor motion, an accurate radial rotor velocity measurement is needed. A measurement of the rotor displacement however would also be sufficient as the velocity is simply obtained with the time derivative of the displacement. Rotor displacements to be measured are in the order of $0.1 \ldots 10\ \mu\mathrm{m}$ and velocities are in the order of $1 \ldots 100\ \mathrm{mm/s}$, which are both very small quantities. Measuring directly the velocities requires observation of the back electromotive force (EMF) which is proportional to the radial velocity and therewith a very small quantity compared to the self-induced voltage resulting from the injected damper current. Hence very accurate models would be needed to successfully apply observer based control. Therefore, although the hardware effort on the control electronics and sensing side would be very small, back electromotive force based self-sensing, as used in [11] for vibration control of a non-rotating structure, is considered too susceptible to modeling errors especially when high bandwidth needs to be achieved. Accordingly, this method is not analyzed further.

Another method commonly used with self-sensing magnetic bearings is the measurement of the winding inductance, which is a function of magnetic air-gap and hence the displacement. The bearings linear power amplifier or switched amplifier is therewith used to modulate the bearing current or superimpose a test signal in order to observe the inductance change [12], [13]. In the present machine however, no ferromagnetic materials are used on the rotor, for which reason no change of the self inductance occurs and the method cannot be applied.

Commonly used sensors proven useful in magnetic bearing systems are eddy current sensors [14],[15]. Furthermore, they are not restricted to only ferromagnetic materials. For the presented magnetic damper a concept is proposed, where the damper coils, which are implemented as air-gap windings, are simultaneously used as eddy current displacements sensors. To obtain high sensitivity of the eddy current displacement measurement, injection of a sinusoidal test signal with a frequency of up to $10\ \mathrm{MHz}$ is required. Signal injection at such a high frequency cannot be easy accomplished by the linear or switched power amplifier used for the damper current, such that a separate signal injection and measurement circuit is required. Finally, the velocity measurement needed for generating a damping force is obtained from the time derivative of the measured displacement. As only the time derivative is used, a probable misalignment of the coils in respect to the bearing bushes or the rotor center, which results in a static offset error in the displacement measurement, has no impact on the damper performance.

For the heteropolar magnetic damper, a winding with two pole pairs such as proposed in [16] for a high-speed active magnetic bearing could be used. Together with the same diametrically magnetized permanent magnet as already needed for torque generation damping force are then obtained. With

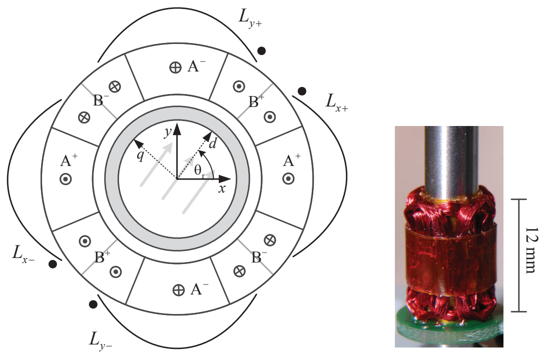


(a) (b)

Fig. 5. (a) Winding scheme of the heteropolar two-phase magnetic damper winding with separated coils for high frequency signal injection position sensing. The dots designates the winding sense of the coils. (b) Prototype winding.

such a skewed winding, vibrations can be controlled if the journal displacement or velocity is known by means of additional sensors. However, because of lacking possibilities for additional tappings for signal injection and measurement, the skewed winding is not suited for journal position self-sensing when using a high frequency signal injection approach.

Therefore, a straight winding with paired coils in each phase on opposite sides would be more convenient for signal injection self-sensing. The number of phases needs to be chosen $m \geq 2$. In order to obtain position information in both radial directions $x$ and $y$, phase symmetric test signals need to be injected into the windings. Phase symmetric sinusoidal signal injection can be achieved by realizing a multi-phase oscillator using the winding coils and additional capacitors as resonant tanks in order to obtain large amplitude measurement signals as an effect of resonance. Otherwise signal injection can also be accomplished by generating the phase shifted sinusoidal or possibly also rectangular signals by means of a digital signal processor and appropriate drivers.

As the sensing circuit complexity for both signal injection and measurement is increased with the number of phases, the special case of the winding with a minimal number of $m = 2$ phases is chosen for a first analysis. A possible configuration of such a winding for the heteropolar damper is depicted in Fig. 5. Phase $A$ is implemented as an ordinary series connection of the winding turns to be summarized as a single coil $L_A$. Phase $B$ is split into four coils $L_{x+}$, $L_{x-}$, $L_{y+}$ and $L_{y-}$, each with tappings, which finally have to be connected in series to conduct the damper current from the power amplifier. Naturally the order of the series connection is of no importance for the force generation, hence the coil order within the series connection can be chosen to be suited for position sensing.

The impedances of the coils $L_{x+}$, $L_{x-}$, $L_{y+}$ and $L_{y-}$ can be described as

$$Z_{x+} = Z - \Delta Z_x \tag{7}$$

$$Z_{x-} = Z + \Delta Z_x \tag{8}$$

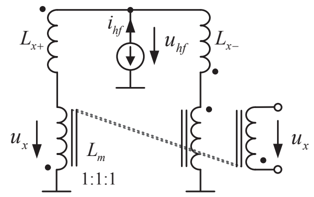


Fig. 6. Bridge connected windings $L_{x+}$ and $L_{x-}$ for the measurement of the displacement dependent impedance change using additional coupled inductors.

$$Z_{y+} = Z - \Delta Z_y \tag{9}$$

$$Z_{y-} = Z + \Delta Z_y, \tag{10}$$

where $Z$ is the coil impedance for a perfectly centered rotor and $\Delta Z_x$ and $\Delta Z_y$ represent the impedance change due to the displacements in $x$ and $y$ directions, $\varepsilon_x$ and $\varepsilon_y$.

It is to be noted that in a first order approximation the impedance $Z_{x+}$ and $Z_{x-}$ only depends on the displacement $\varepsilon_x$ and $Z_{y+}$ and $Z_{y-}$ depend only on the displacement $\varepsilon_y$. Therefore the coils can be used independently in pairs, $L_{x+}$ and $L_{x-}$ for the sensing of $\varepsilon_x$ and $L_{y+}$ and $L_{y-}$ for the sensing of $\varepsilon_y$.

To measure the impedance change a measurement bridge as depicted in Fig. 6 is applied. Unlike with a conventional Wheatstone bridge, no differential voltage measurement is needed. Instead, the common mode voltage is canceled with the use of differentially coupled inductors. Assuming ideal inductors $L_m$ without a parasitic series resistance, the voltage across the inductor measured to ground

$$u_x = i_{hf} \cdot \frac{Z_m}{Z + 2Z_m} \cdot \Delta Z_x \tag{11}$$

is directly proportional to the impedance change $\Delta Z_x$. However with a parasitic series resistance, an offset would be present for which reason the voltage $u_x$ is better measured on the terminals of a third coupled winding.

Fig. 7 shows a possible combination of the required series connection of the winding coils with the measurement bridge. The high frequency currents $I_{hf} \cos \omega t$ and $I_{hf} \sin \omega t$ are injected capacitively through $C_{in}$, which is necessary for two reasons. First, the damper current from the power amplifier is not supposed to be influenced at low frequencies and second, the signal injecting buffers need to be decoupled from the mid-point of the windings which otherwise would expose the buffers to the high back-EMF voltage at high rotational speeds. A further additional capacitor $C_m$ is added which represent a short circuit for the high frequency signal. The output of the power amplifier for phase $B$ also needs to exhibit low impedance at high frequencies whereby together with $C_m$ the measurement bridge is obtained. The capacitor $C_m$ has to be dimensioned not to affect the current from the power amplifier at low frequencies.

To obtain the displacements, the signals $u_x$ and $u_y$ are fed through a bandpass filter. Then a frequency mixer is used as commonly done for demodulation (e.g. in [17]). The mixer

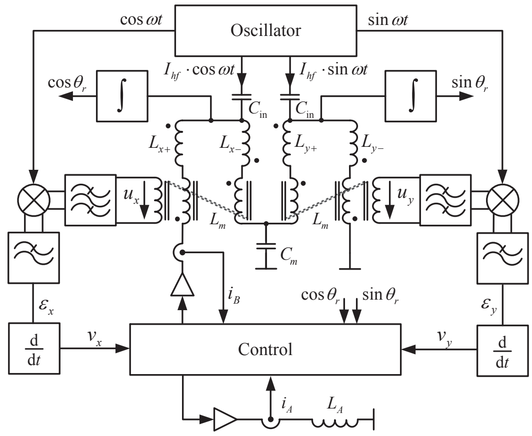


Fig. 7. Self-sensing high frequency signal injection circuit for displacement measurement in $x$ and $y$ directions ($\varepsilon_x$ and $\varepsilon_y$) with power amplifiers and control.

is followed by a low-pass filter, which eliminates the high frequency spectral components and yields a signal which is proportional to the displacements $\varepsilon_x$ and $\varepsilon_y$. The displacement signals are then further processed to obtain the radial velocities needed for the control of the damper currents.

In order to transform the damper reference currents from the rotating $dq$-coordinate system of the rotor into winding reference currents, also the angular rotor position $\theta_r$ needs to be measured. The winding reference currents are then given by

$$i_A^* = i_d^* \cos \theta_r - i_q^* \sin \theta_r \tag{12}$$

$$i_B^* = i_d^* \sin \theta_r + i_q^* \cos \theta_r. \tag{13}$$

Therefore the back-EMF at the winding mid-point is tapped and integrated yielding $\cos \theta_r$ and $\sin \theta_r$ which are proportional to the permanent magnet flux in $x$ and $y$ directions and can be directly used for the above transformation.

## IV. Sensitivity Measurement

The winding specifications for the test setup are given in Tab. I. For the rotor a 6 mm stainless steel rod (1.4301) is used. A high frequency current with amplitude $I_{hf} = 20$ mA is injected into the winding and the voltage $U_x$ is measured at the output of the measurement bridge (Fig. 6). For the coupled inductor $L_m$ a double-aperture core (Epcos K1) with an inductance of $3 \times 10$ $\mu$H is used. Fig. 8 shows the measured output voltage $U_x$ normalized with the injected current $I_{hf}$ as a function of the rotor displacement $\varepsilon_x$ for various frequencies. If the voltage $U_{hf}$ is also measured, the relative impedance change of the winding can be determined as

$$\frac{\Delta Z_x}{Z} = \frac{U_x(I_{hf} Z_m + U_{hf})}{U_x^2 + I_{hf} Z_m U_{hf}}. \tag{14}$$

The obtained impedance change as a function of the rotor displacement $\varepsilon_x$ is plotted in Fig. 9. At a frequency of 10 MHz the relative impedance change is approximately 0.1% per micrometer. The sensitivity of winding with the proposed

TABLE I
DAMPER WINDING SPECIFICATIONS

| | |
|---|---|
| Inner diameter | 6.5 mm |
| Outer diameter | 8.5 mm |
| Length | 12.0 mm |
| Number of turns (per coil side) | 20 |
| Inductance phase $A$ (10 kHz) | 25 $\mu$H |
| Inductance phase $B$ (10 kHz) | $4 \times 5.6$ $\mu$H |
| Resistance phase $A$ | 4.6 $\Omega$ |
| Resistance phase $B$ | $4 \times 1.2$ $\Omega$ |
| Force-current constant $K_I$ | 0.46 N/A |

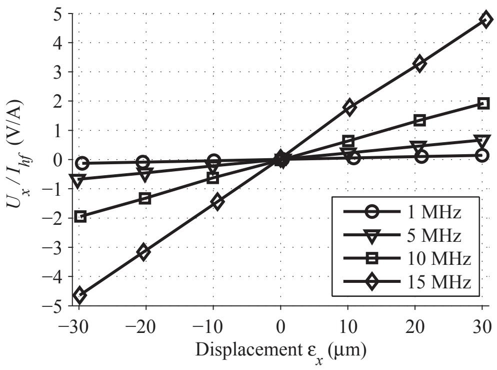


Fig. 8. Measurement bridge output voltage $U_x$ normalized with the injected current $I_{hf}$ as a function of the rotor displacement $\varepsilon_x$.

measurement bridge is over 100 times higher than the eddy current sensor for AMBs analyzed in [18] and therefore it is considered high enough to resolve the journal movement with high precision in order to obtain accurate vibration control.

## V. Conclusion

In order to enable the use of ultra high-speed electrical drive systems with high reliability and long lifetime in industrial applications, a new hybrid bearing concept employing a gas bearing in combination with a small-sized active magnetic damper has been proposed. Without compromising the high load capacity or stiffness of the gas bearing, the magnetic damper is used to effectively facilitate dynamic stability at high rotational speeds. A conceptual design with initial numerical estimates and has been presented to show the feasibility of the hybrid approach. Furthermore, experimental results of the position measurement have been presented. With the proposed twofold use of the existing permanent magnet and the application of a high frequency signal injection position self-sensing method, the amount of additional components is minimized yielding a drive system with a only few additional components resulting in low extra system complexity and costs.

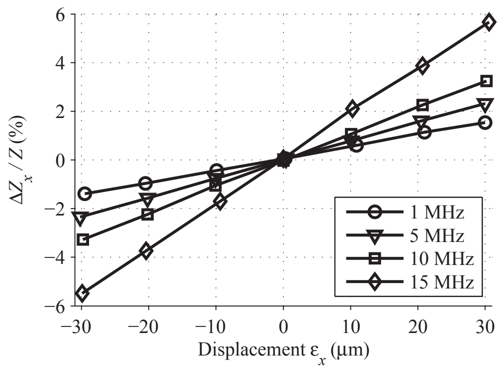


Fig. 9. Impedance change $\Delta Z_x$ of a damper winding coil related to its total impedance $Z$ as a function of the rotor displacement $\varepsilon_x$.

## References

[1] H. Marsh, "The stability of aerodynamic gas bearings," *Mechanical Engineering Science Monograph*, vol. 2, June 1965.
[2] D. Kim and D. Lee, "Design of three-pad hybrid air foil bearing and experimental investigation on static performance at zero running speed," *Journal of Engineering for Gas Turbines and Power*, vol. 132, no. 12, p. 122504, 2010.
[3] D. Flemming and B. Hamrock, "Optimization of self-acting herringbone journal bearings for maximum stability," in *6th International Gas Bearing Symposium*, March 1974.
[4] M. Salehi, H. Heshmat, J. F. Walton, and M. Tomaszewski, "Operation of a mesoscopic gas turbine simulator at speeds in excess of 700,000 rpm on foil bearings," *Journal of Engineering for Gas Turbines and Power*, vol. 129, no. 1, pp. 170–176, 2007.
[5] T. Waumans, J. Peirs, F. Al-Bender, and D. Reynaerts, "Aerodynamic journal bearing with a flexible, damped support operating at 7.2 million DN," in *PowerMEMS*, November 2010, pp. 199–202.
[6] A. El-Shafei and A. S. Dimitri, "Controlling journal bearing instability using active magnetic bearings," *Journal of Engineering for Gas Turbines and Power*, vol. 132, no. 1, p. 012502, 2010.
[7] J. Luomi, C. Zwyssig, A. Looser, and J. W. Kolar, "Efficiency optimization of a 100-W, 500 000-rpm permanent-magnet machine including air friction losses," in *Proceedings of IEEE 42nd IAS Annual Meeting Industry Applications Conference (IAS '07)*, 2007, pp. 861–868.
[8] G.Schweitzer and E. Maslen, *Magnetic bearings - theory, design, and application to rotating machinery*. Springer, 2009.
[9] T. Baumgartner, A. Looser, C. Zwyssig, and J. Kolar, "Novel high-speed, Lorentz-type, slotless self-bearing motor," in *Energy Conversion Congress and Exposition (ECCE), 2010 IEEE*, September 2010, pp. 3971 –3977.
[10] J. Vohr and C. Chow, "Characteristics of herringbone-grooved, gas-lubricated journal bearings," *Journal of Basic Engineering*, vol. 87, no. 3, pp. 568–578, 1965.
[11] C. Paulitsch, P. Gardonio, and S. J. Elliott, "Active vibration damping using self-sensing, electrodynamic actuators," *Smart Materials and Structures*, vol. 15, no. 2, p. 499, 2006.
[12] L. Kucera, "Zur sensorlosen Magnetlagerung," Ph.D. dissertation, ETH Zurich, Switzerland, 1997.
[13] A. Schammass, R. Herzog, P. Buehler, and H. Bleuler, "New results for self-sensing active magnetic bearings using modulation approach," *Control Systems Technology, IEEE Transactions on*, vol. 13, no. 4, pp. 509 – 516, July 2005.
[14] J. Zoethout, "Design and integration of position sensing systems," Ph.D. dissertation, EPFL, Lausanne, 2002.
[15] R. Larsonneur and P. Buehler, "New radial sensor for active magnetic," in *Magnetic Bearings, 2004. Proceedings., 9th International Symposium on*, 2001.
[16] A. Looser, T. Baumgartner, C. Zwyssig, and J. Kolar, "Analysis and measurement of 3D torque and forces for permanent magnet motors with slotless windings," in *Energy Conversion Congress and Exposition (ECCE), 2010 IEEE*, September 2010, pp. 3792 –3797.
[17] K. Morita, T. Yoshida, and K. Ohniwa, "Improvement of sensing characteristics of self-sensing active magnetic bearings," *Electrical Engineering in Japan*, vol. 166, no. 2, pp. 70–77, 2009.
[18] A. Muesing, C. Zingerli, and J. W. Kolar, "PEEC-based numerical optimization of compact radial position sensors for active magnetic bearings," in *Proceedings 5th CIPS Conference*, 2008.